USING THE O_3/NOY RATIO TO ASSESS THE O_3-NOX-VOC SENSITIVITY IN A WESTERN MEDITERRANEAN COASTAL ENVIRONMENT

Ariel F. Stein*

Centro de Estudios Ambientales del Mediterraneo (CEAM), Valencia, Spain.

1. INTRODUCTION

It is widely known that the formation of ozone (O_3) is chemically linked to the emissions of nitrogen oxides (NOx) and volatile organic compounds (VOC). This chemical interdependence is highly complex and gives rise to non-linear and coupled pollutant formation processes. Measurements and modeling of the levels of key photochemical compounds, such as O_3 and NOy, can provide a set of tools to establish the sensitivity of O_3 to changes in its precursors emissions (Sillman, 1995). Indeed, afternoon O_3/NOy ratios have been widely used as indicators to assess the effectiveness of VOC or NO_x controls in decreasing O_3 abundance in many parts of the world (Sillman et al., 1990, 1997; Martilli et al., 2002). Values for these photochemical indicators higher than a certain threshold, determined by photochemical simulations and literature values, have been related to NOx-sensitive ozone formation (i.e. O_3 is reduced as NOx emissions are reduced and no sensitivity is observed for changes in VOC), while lower levels of the indicator have been linked to a VOC-sensitive regime (i.e. O_3 decreases as VOC emissions are reduced and would even increase if NOx sources strength is lowered).

In this work, two summertime cases have been analyzed to determine the O_3/NOy threshold values for the transition between NOx- and VOC-O_3-sensitivity. The first case involves NOy and O_3 airborne measurements taken downwind the area of Castellon, located on the Mediterranean coast of the Iberian Peninsula. Moreover, the concentrations of these indicator species have been calculated from a series of simulations using a lagrangian photochemical model (RPM-IV). In the second case, O_3 concentrations taken from the local network in the area of Valencia, Spain, have been simulated using a 3-D eulerian model (CMAQ). The sensitivity of ozone to changes in its primary sources has been examined by simulating

scenarios with varying rates of NO_x and VOC emissions for each separate case.

2. METHODOLOGY

2.1 Field Measurements

Case 1: July 27, 1989

Meteorological and chemical data have been measured from an instrumented aircraft (Hawker Siddeley 125 F400B (HS-125)). The gas-phase chemical components that have continuously been measured through this campaign are O_3, sulfur dioxide (SO_2), and NO_y (Millán et al., 1992). An instrumented flight took place around the Castellón urban-industrial area, located on the Mediterranean coast of the Iberian Peninsula (Fig. 1). The flight covered the midfield (within a 75-km radius) of the urban-industrial complex located by the coast and lasted from 15:09 to 15:55 UTC.
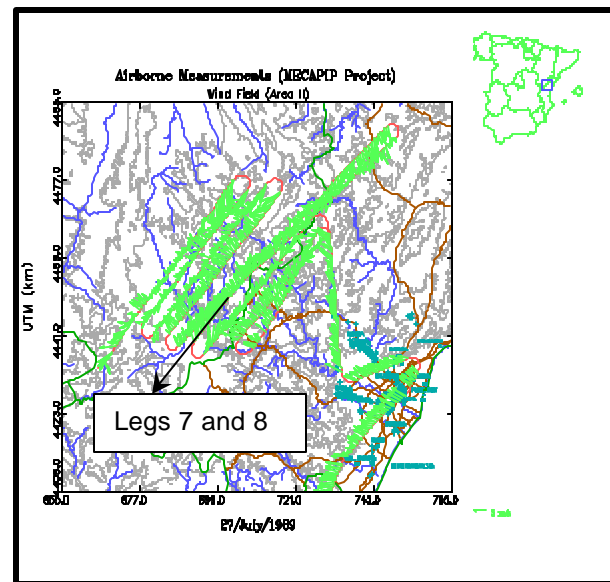

Figure 1: Flight pattern and wind vectors for midfield region downwind Castellón. The map of Spain on the sides shows the areas covered by the flight.

Case 2: August 14, 2005

Analysis of the air quality network in the Valencia Community (VC) has shown that the human health protection threshold for ozone (120

*Corresponding author: Ariel F. Stein, Centro de Estudios Ambientales del Mediterraneo (CEAM). C. Darwin 14. Parque Tecnologico de Paterna, Valencia, 46980, Spain; e-mail: astein@ceam.es

μg/m3 8-hour average) has been systematically exceeded almost every day between March and September. Moreover, the vegetation protection threshold (AOT40 18000 μg/m3) has also been surpassed. Since 1999, heuristic models, and more recently photochemical ones, have been applied to analyze such ozone exceedances. In particular, an ozone episode that took place during the period of August 13-14, 2000 in the Eastern Spanish coast, including Valencia community, has been examined.

2.2 Model Description

Case 1: July 27, 1989

The main processes responsible for the formation of ozone have been simulated using the Reactive Plume Model IV (RPM-IV) (Morris *et al.*, 1992). This model depicts the complex interaction of plume dispersion and nonlinear plume photochemistry. The RPM-IV uses the Lagrangian approach to describe a vertically well-mixed and horizontally segmented air parcel as it moves downwind with the wind speed, simulating the contribution from emission sources along the trajectory of the plume, the horizontal dispersion and mixing between adjacent segments, the horizontal entrainment of ambient air, and the resulting photochemical transformations. This model simulates the chemical evolution of pollutant species during transport and dispersion, but does not solve the nonlinear hydrodynamic equations for fluid flow.

Case 2: August 14, 2000

In order to understand the observed spatial and temporal variations in ozone levels, the Community Multiscale Air Quality (CMAQ) (EPA, 1999) modeling system with meteorological fields obtained from Mesoscale Model Version 5 (MM5) (Dudhia, 1993) has been utilized to simulate air quality in the VC.

3. CASE STUDIES

3.1 Meteorological Conditions

Case 1: July 27, 1989

Airborne measurements have been carried out under summertime atmospheric conditions, associated with the presence of an Atlantic high-pressure system, well established at mid-latitudes and extending to central Europe and the Western Mediterranean. Moreover, a high-level pressure ridge reinforces this system. The pollutants measured during the flights have been emitted into an atmosphere relatively confined by the presence of at least one inversion layer. This coastal thin layer extends to about 800 m at its maximum development stage. It is expected, however, to grow higher inland (to approximately 1000 m). During the airborne sampling, the wind field pattern shows a well-defined easterly circulation.

Case 2: August 14, 2000

Meteorological conditions corresponding to this episode feature a weak pressure gradient along with a relative low-pressure development in the southern part of the peninsula (Iberian Thermal Low). Under these synoptic conditions and induced by the local characteristics of the terrain, mesoscale flow features, such as land and sea breezes, mountain wind and topographic injection, develop.

3.2 Simulation of the Episodes

Case 1: July 27, 1989

Primary emissions of NOx, VOC, and carbon monoxide (CO) have been calculated based on a local emissions inventory (Martín *et al.*, 1998). This inventory includes mobile, area, and point (power plant and industrial) sources and encompasses the area of Castellon with a resolution of 1 km^2. Isoprene and other biogenic species emissions have been estimated using local land use, radiation, and biogenic emission factors (Guenther *et al.*, 1993; 1995). The Carbon Bond Mechanism IV (CBM-IV) (Gery *et al.*, 1989) has been used to describe the gas-phase chemical processes that occur within each segment of the plume.

All simulations begin at 12:00 UTC at the coast of the Mediterranean and extend for 4 hours (ending at 16:00 UTC). Air parcels departing from the coast line travelling at an estimated average wind speed of 4 ms^{-1} will cover a distance of 58 km in 4 hours, approximately. Consequently, only the left half of legs 7 and 8 (Figure 1), located at about 57 km from the coast, have been chosen for this modeling exercise. The left half of these legs have been selected to assure that the sampled air mass only contains pollutants that have been originated from the Castellon urban-industrial complex. Also, these are the only transects that allow the model to be initialized with airborne measurements taken from a noon near-field flight sampling at the coast line. In particular, the O_3 concentration has initially been set to 65 ppb while the rest of species have been set to background values (i.e. NOx = 1.5 ppb, CO = 300 ppb, VOC =

2

15 ppb). Boundary conditions for horizontal entrainment have been calculated using only one segment of the model (as a box model) with the same initial conditions but without any emission sources injected into the box.

Five horizontal segments with a starting width of 1 km each, coinciding with the horizontal resolution of the emissions, have been chosen to depict the left half of the travelling air parcel reaching the left half of legs 7 and 8 (Figure 1) at 16:00 UTC. These segments horizontally expand as the parcel moves inland ingesting different pollutants emitted by a variety of sources such as a power plant, the city of Castellon, mixed industries, and biogenic emissions. The modeled air parcels have been made to follow the trajectory calculated by assuming the airborne measured winds were steady state.

Case 2: August 14, 2000

The non-hydrostatic MM5 v3.5 model has been used to simulate the meteorological pattern. The simulation has been initialized at 00UTC 13 August 2000 and run through 1800 UTC 16 August 2000. Four nested grids have been used with 2, 6, 24, and 72 km horizontal resolution and a variable vertical resolution ranging from 0 to 15 km, with 10 m on the first level.

Emission calculations have been performed to account for primary pollutants released from sources located in two different domains, the first domain covering the Iberian Peninsula and the second one the Valencia Community. Sources corresponding to the Iberian Peninsula have been estimated based on EMEP emissions inventory. On the other hand, a high-resolution emission inventory has been developed for this VC region, including the estimation of biogenic and road-traffic emissions. These emission sources have been calculated with a 1-h temporal and 1 km^2 horizontal resolution using a bottom-up approach for primary pollutants (NO_X, VOC, and CO).

The CMAQ model version 4.22 has been implemented using the pierce-wise parabolic method (PPM) for advection, K-theory parameterization for vertical diffusion, Carbon Bond IV (CB-IV) chemistry mechanism, and quasi-steady state approximation (QSSA) gas-phase reaction solver. Meteorological output data from MM5 has been linked to CMAQ utilizing the Meteorological Chemistry Interface Processor (MCIP). Two nested grids have been defined, a coarse grid with 24 km horizontal resolution (50x46 cells) covering the Iberian Peninsula and a fine grid with 4 km horizontal resolution (172x108 cells) encompassing the VC. The number of vertical layers is 15.

4. MODEL EVALUATION

Case 1: July 27, 1989

The RPM-IV model depicts the range and magnitude of the O_3 and NOy airborne measurements (Figure 2). Measured ozone concentrations are predicted within 5%. The model predicts NOy with a normalized bias of less than 10%.
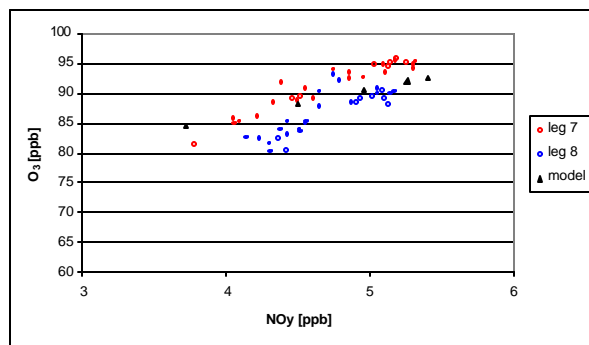

Figure 2: Measured and modeled O_3 vs NOy corresponding to left half of flight legs 7 and 8.

Case 2: August 14, 2000

Ozone levels measured at 6 monitoring stations have been compared with CMAQ model outputs (Figure 3). CMAQ reproduces the main qualitative features of the temporal evolution of ozone. Good quantitative representation of the patterns is observed for stations located on the central and southern portions of the VC domain (Puerto Sagunto, Paterna, and Renfe). However, the model tends to underpredict the ozone levels at stations (Grao, Zorita, and Morella) influenced by industrial sources that have not been included among the emission estimates.

5. O3-NOx-VOC SENSITIVITY

In order to investigate the O_3 sensitivity to changes in primary precursor emissions the two scenarios have been run with 50% and 35% reductions in emissions rates separately for NOx and anthropogenic VOC, respectively. Figure 4 shows the percentage normalized reduction in O_3 as a consequence of either a NOx or a VOC emission reduction for all the anthropogenic sources simulated. The change in O_3 has been plotted as a function of the concurrent indicator ratio, O_3/NOy (Figure 4). As can be inferred, there is a well-defined contrast between NOx and VOC sensitive locations. Values higher than a certain
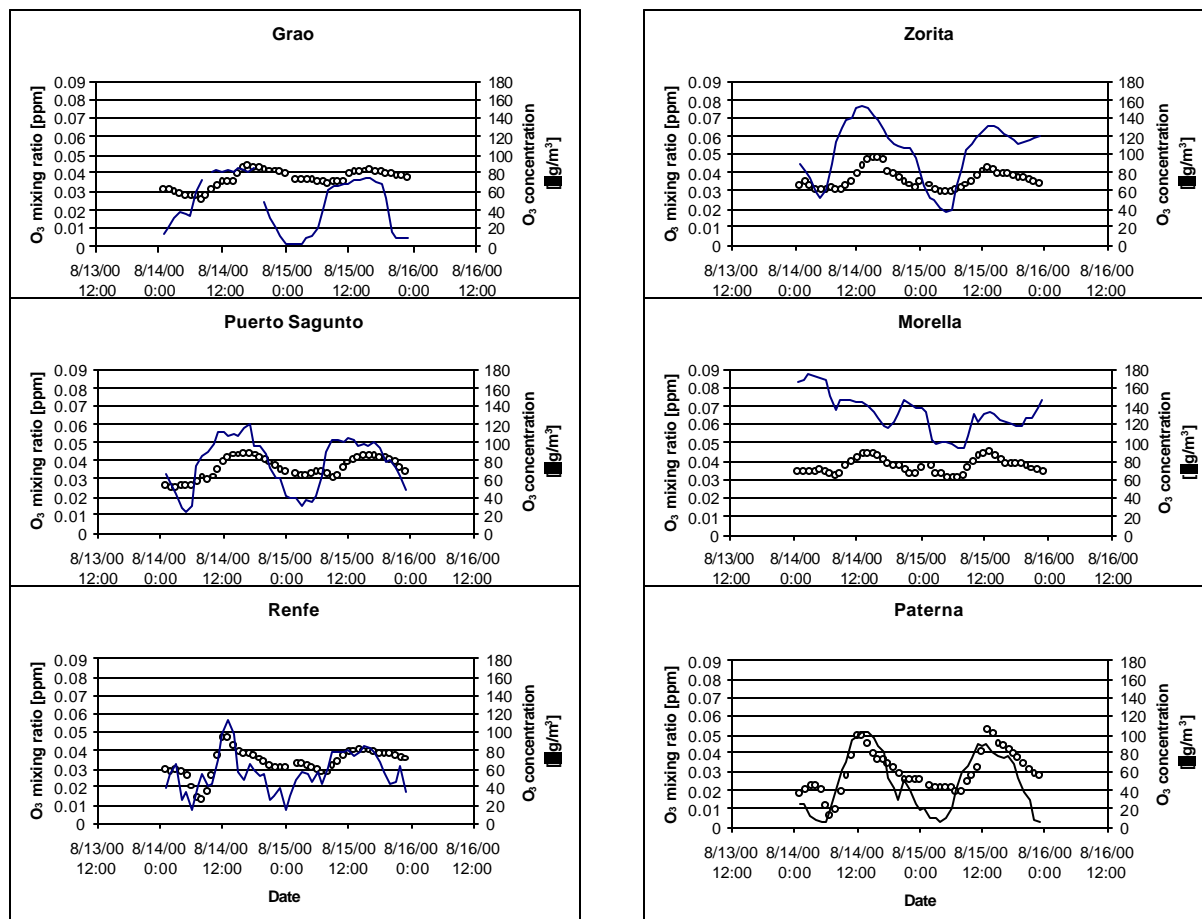
Figure 3: Comparison of measured (line) and modeled (circles) hourly ozone concentrations as a function of time for some representative stations in the Valencia community.

threshold for the O_3/NOy ratio can be related to NOx-sensitive ozone formation while lower values are associated to VOC-sensitive conditions.

The correspondence between the O_3-NOx-VOC sensitivity and the indicator ratio has been evaluated quantitatively by calculating the distribution of the populations for the O_3/NOy ratios associated with VOC- and NOx- sensitive locations respectively. We define NOx-sensitive locations as those where the normalized O_3 calculated in the simulation with a reduction in NOx is lower than the normalized ozone concentrations modeled with reductions in VOC by at least 2%. VOC locations are defined in an analogous way. Table 1 shows that the median values of the O_3/NOy ratios linked to NOx-sensitive locations are at least three times higher than those associated with VOC-sensitive locations. The 95th percentile of the collection of indicator values corresponding to VOC-sensitive stations along with the 5th percentile of indicator values associated with NOx-sensitive locations identify the threshold interval of the transition from VOC- to NOx-sensitivity.

	VOC sensitive			NOx sensitive		
Percentile	5th	50th	95th	5th	50th	95th
O_3/NOy (**case 1**)	1.6	5.1	9.2	12.9	17.5	23.2
O_3/NOy (**case 2**)	3.3	8.2	12.5	12.9	26.1	53.6
NE corridor, USA (Sillman and He,2002)	5.0	5.4	6.5	8.2	12.7	18.0
Lake Michigan, USA (Sillman and He,2002)	3.5	5.2	6.6	7.2	11.7	16.0
Atlanta, USA (Sillman et al, 1997)	3.6	5.1	7.2	8.1	14.3	27.0
San Joaquin, USA (Sillman and He,2002)	3.0	7.3	11.6	15.0	26.0	56.0
Milan, Italy (Martilli et al., 2002)	3.6	4.3	5.6	5.7	8.2	11.1

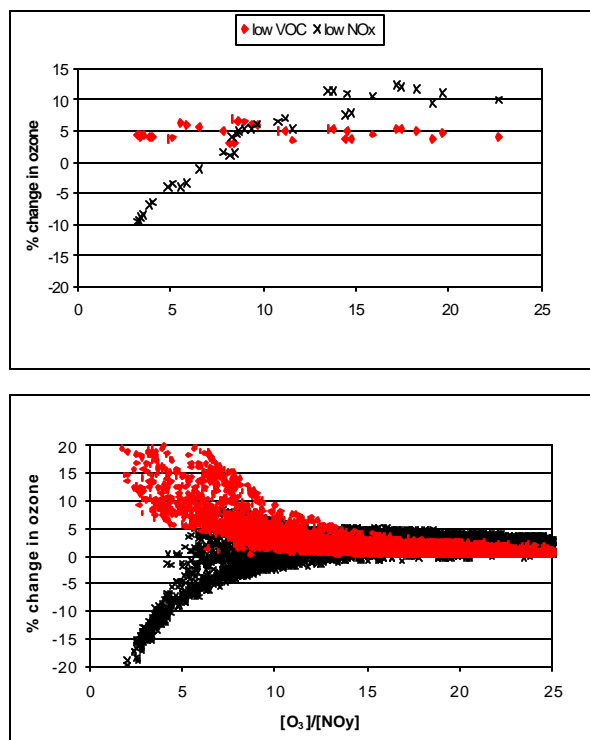Table 1: Distribution of O_3/NOy ratios for NOx- and VOC- sensitive regimes.

4

Fig. 4. Normalized percentage response of O_3 concentrations to changes in NOx and VOC versus O_3/NOy corresponding to cases 1 and 2, respectively.

The calculated value of the O_3/NOy ratio for the transition from NOx- to VOC-sensitivity is somewhat higher than those calculated in previous studies (Table 1), with the exception of San Joaquin, USA. Sillman and He (2002) noticed that the NOx-VOC transition depends on the O_3 levels for indicators such as the O_3/NOy ratio. Furthermore, higher transition values have been associated with lower ozone levels due to the uncertainty in regarding O_3/NOy as a surrogate to the ratio of the source of odd hydrogen to the source of odd nitrogen when calculating the threshold ratios (see Sillman and He (2002) for a detailed explanation). For moderately polluted environments (100-200 ppb O_3) the separation from NOx- to VOC-sensitive locations ranges 6-8 for the O_3/NOy ratio, while for O_3 less than 80 ppb the change in indicator transition value is higher (O_3/NOy = 11-15) (Sillman and He, 2002). Considering that the O_3 levels measured and simulated in this study are between 80 and 100 ppb then the transition values obtained (O_3/NOy = 9 – 13) appear to be consistent with Sillman and He's findings.

6. CONCLUSIONS

Two summertime cases have been analyzed to determine the O_3/NOy threshold values for the transition between NOx- and VOC- O_3-sensitivity. The first case involves NOy and O_3 airborne measurements taken downwind the area of Castellon, located on the Mediterranean coast of the Iberian Peninsula. Moreover, the concentrations of these indicator species have been calculated from a series of simulations using a lagrangian photochemical model (RPM-IV). In the second case, O_3 concentrations taken from the local network in the area of Valencia, Spain, have been simulated using a 3-D eulerian model (CMAQ). The sensitivity of ozone to changes in its primary sources has been examined by simulating scenarios with varying rates of NO_x and VOC emissions for each separate case. The results presented here show that the threshold value for the O_3/NOy ratio is somewhat higher than those found in other environments (9-12 in this work in contrast to 6-8 in the NE USA). This higher threshold value seems to be associated to the lower ozone levels observed in the Western Mediterranean area (70-100 ppb) and to the uncertainty in regarding O_3/NOy as a surrogate to the ratio of the source of odd hydrogen to the source of odd nitrogen when calculating the threshold ratios.

7. REFERENCES

EPA, 1999. Science Algorithms of the EPA MODELS-3 Community Multiscale Air Quality (CMAQ) modeling system, Rep. EPA/600/R-99/030, Off. Of Res. And Dev., Washington, D.C.

Dudhia, J., 1993: A non-hydrostatic version of the Penn State-NCAR mesoscale model: Validation tests and simulation of an Atlantic cyclonic and cold front. *Monthly Weather Review* 121, 1493-1513.

Gery, M.W., Whitten, G.Z., Killus, J.P, and Dodge M.C., 1989. A photochemical kinetics mechanism for urban and regional scale computer modeling. Journal of Geophysical Research 94 (D10), 12925-12956.

Guenther A.B., Zimmerman, P.R., Harley, P.C., Monson, R.K., and Fall, R., 1993. Isoprene and monoterpene emission rate variability: Model evaluations and sensitivity analyses Journal of Geophysical Research 98 (D7), 12609-12617.

Guenther A.B., Hewitt, C.N., Erickson, D., Fall, R., Geron, C., Graedel, T., Harley, P.C., Klinger, L., Lerdau, M., McKay, W.A., Pierce, T., Scholes, B., Steinbrecher, R., Tallamraju, R., Taylor, J., and Zimmerman, P.R., 1995. A global model of natural volatile organic compound emissions. Journal of Geophysical Research 100 (D5), 8873-8892.

Martilli, A., Neftel, A., Favaro, G., Kirchner, F., Sillman, S., and Clappier, A., 2002. Simulation of the ozone formation in the northern part of the Po Valley. Journal of Geophysical Research 107 (D22), 8195 doi: 10.1029/2001JD000534.

5

Martín F., Palacios, M., Cabal, H., Gómez, M., Domínguez, J., Sánchez, I., Salazar M.J., and Salvador, R., 1998. Anthropogenic emission inventory around the city of Burriana (Valencia). *Report CIEMAT nº 11320-96-11-F1PE-ISP*.

Millán M.M, Artiñano, B., Alonso, L., Castro, M., Fernandez-Patier, R., and Goberna, J., 1992. Mesometeorological Cycles of Air Pollution in the Iberian Peninsula, *Report Air Pollution Research Report 44*, Commission of the European Communities, contract EV4V-0097-E.

Morris, R.E., Chang, E.C., Wang, Z.S., Shepard, S.B., and Ligocki M.P., 1992. User's Guide Reactive Plume Model IV (RPM-IV). SYSAPP-92/123. Contract 68-D90066. Systems Applications International.

Sillman S., 1995. The use of NO_y, H_2O_2, and HNO_3 as indicators for ozone-NO_x-hydrocarbon sensitivity in urban locations. Journal of Geophysical Research 100 , 14175-14188.

Sillman S., He., D., Cardelino, C., and Imhoff, R.E., 1997. The use of photochemical indicators to evaluate ozone-NO_x-Hydrocarbon sensitivity: Case studies from Atlanta, New York, and Los Angeles. Journal of the Air and Waste Management Association 47, 1030-1040.

Sillman S., and He, D., 2002. Some theoretical results concerning O3-NOx-VOC chemistry and NOx-VOC indicators. Journal of Geophysical Research 107 (D22), 4659, doi:10.1029/2001JD001123.

Sillman S., Logan, J.A., and Wofsy, S.C., 1990. The sensitivity of ozone to nitrogen oxides and hydrocarbons in regional ozone episodes. Journal of Geophysical Research 95, 1837-1851.